

Effect of Shrinkage on Thermal Restrained Strain in Mass Concrete

Jiranuwat Banjongrat *

School of Civil Engineering and Technology,
Sirindhorn International Institute of Technology, Thammasat University
Rangsit Campus, Khlong Nueng, Khlong Luang, Pathum Thani 12120, Thailand

Krittiya Kaewmanee

Construction and Maintenance Technology Research Center (CONTEC),
Sirindhorn International Institute of Technology, Thammasat University
Rangsit Campus, Khlong Nueng, Khlong Luang, Pathum Thani 12120, Thailand

Somnuk Tangtermsirikul

School of Civil Engineering and Technology,
Sirindhorn International Institute of Technology, Thammasat University
Rangsit Campus, Khlong Nueng, Khlong Luang, Pathum Thani 12120, Thailand

Abstract

The aim of this study is to simulate restrained strain of mass concrete at early age due to combined thermal effect and shrinkages. Firstly, restrained strain caused by differential thermal expansion as well as restrained strains caused by shrinkages are separately computed. Thermal properties such as specific heat, thermal conductivity and thermal expansion coefficient of concrete are estimated by the authors' mathematical models. The previously proposed adiabatic temperature rise model is used to calculate heat of hydration. Heat of hydration obtained from the modified adiabatic temperature rise model and thermal properties derived from our proposed models are used as the input in a commercialized three-dimensional finite element program to calculate semi-adiabatic temperature and restrained strain. The restrained strains caused by shrinkages are computed based on our existing mathematical models for estimating free shrinkages. Both autogenous and drying shrinkages are considered. The total restrained strain is subsequently computed by the supercomposition concept. It is found that autogenous shrinkage reduces the thermal cracking risk at early age during the insulation curing period, while after removal of insulation curing material drying shrinkage increases the risk of cracking.

Keywords: mass concrete; semi-adiabatic temperature rise; thermal cracking; drying shrinkage; restrained strain

1. Introduction

Mass concrete has been extensively used for large dimension construction such as dams and mat foundations. In massive concrete structures, the temperature rise due to heat of hydration causes temperature gradients which can induce cracks, especially

at the early age of the concrete. Cracking of massive structures can reduce load carrying capacity or service life of a structure by introducing early deterioration, which can lead to excessive maintenance. To avoid cracking due to heat of hydration, one approach is to control the hydration heat of

*Correspondence : jiranuwat@msn.com

concrete by reducing cement content. Fly ash is one of the pozzolanic materials which can be effectively used as a cement replacing material to reduce the hydration heat of concrete.

Thermal cracking is not the only cause of cracking in mass concrete. In general, mass concrete encounters stresses due to both thermal effect and shrinkages. Since shrinkage is another cause of cracking, its effects should be included in the cracking analysis of mass concrete. Total shrinkage of concrete is mainly composed of autogenous and drying shrinkages. Autogenous shrinkage occurs at early age during the progress of hydration reaction. Drying shrinkage is the volume change due to loss of water from the concrete to the surrounding environment. Shrinkage cracking can take place at either early or later ages. If shrinkage of concrete takes place without any restraint, concrete will not crack. Unfortunately, concrete structures are always subjected to a certain degree of restraint. The conflict between shrinkage and restraint induces restrained strain. When this restrained strain reaches the tensile strain capacity, the concrete cracks. Development of a computerized program for predicting cracking of mass concrete is beneficial to design mix proportion and construction process. Many researchers [1-4] proposed methods for predicting thermal cracking in mass concrete; however, the effect of shrinkage was not considered in their methods.

For this reason, this study incorporates the effect of autogenous and drying shrinkages, with the use of established free autogenous and drying shrinkage prediction models [5], into the thermal cracking analysis to demonstrate their effects and to make the analysis more realistic. It's noted here that this study covers only the case of internally restrained thermal stress.

2. Existing Models

2.1 Semi-adiabatic and Thermal Cracking Model

A flow chart of the proposed model for simulating thermal cracking of mass concrete is shown in Fig.1. Heat of hydration and heat produced by pozzolanic reaction, which were obtained from the models proposed by Saengsoy and Tangtermsirikul [6], were used as the input for a commercial FEM program. Thermal properties such as specific heat, thermal conductivity and coefficient of thermal expansion (CTE) are obtained from the thermal properties model proposed by Choktaweekarn [4]. The FEM program was used to analyze the semi-adiabatic temperature rise of concrete. For the proposed model, three dimensional eight node brick elements were used in the analysis. The couple thermo-mechanical problem was used in the analysis in which heat transfer analysis is solved first. The temperature obtained from the heat transfer analysis is used as the input for the computation of the restrained strain. More details are mentioned below.

2.1.1 Heat Transfer Analysis

By the use of the common heat transfer analysis which was mentioned by many researchers [7-13], together with the derived heat of hydration and pozzolanic reactions and thermal properties from our existing models, the semi-adiabatic temperature can be analyzed.

The governing equation of heat transfer for temperature prediction of mass concrete with consideration of heat of hydration is shown in Eq. (1).

$$\rho c \frac{\partial T}{\partial t} = q_{hy} + \frac{\partial}{\partial x} \left(k_x \frac{\partial T}{\partial x} \right) + \frac{\partial}{\partial y} \left(k_y \frac{\partial T}{\partial y} \right) + \frac{\partial}{\partial z} \left(k_z \frac{\partial T}{\partial z} \right) \quad (1)$$

Where: k_x , k_y , k_z are thermal conductivities of concrete in x, y and z directions, respectively (kcal/m hr °C). ρ is concrete density (kg/m³), c is specific heat of concrete

(kcal/ kg °C), q_{hy} is heat of hydration and pozzolanic reaction (kcal). t is age of concrete (hr.). T is temperature of concrete (°C).

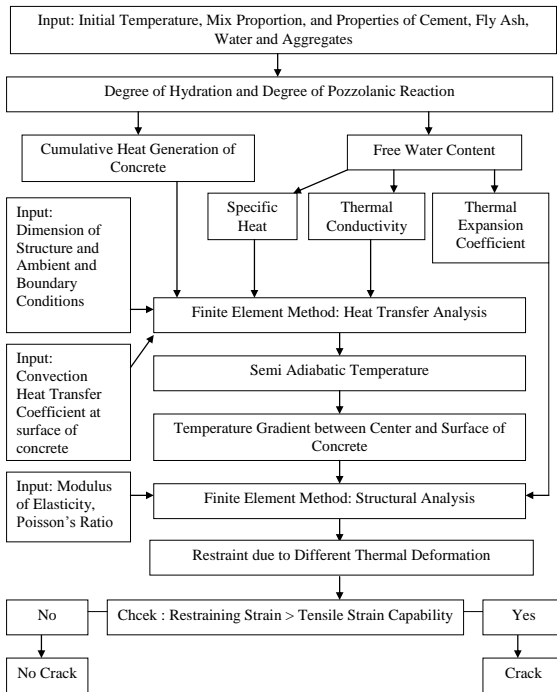


Fig.1. A flow chart of the proposed model for simulating thermal cracking of mass concrete.

The heat transfer inside the concrete mass is governed by Eq. (1); however, the condition at the concrete surface is different. Conduction process plays an important role in transferring heat within the interior elements. However, for exterior elements, convection plays a dominant role in transferring heat at the concrete surface. The presence of wind and solar radiation affect the temperature profile significantly and must be considered. The convective heat transfer is involved in transferring heat between the surface of mass concrete and the environment (between concrete and air). The amount of heat transfer at the surface of concrete can be calculated using Newton's cooling law. For simplicity, radiation is taken into account together with the

convection, through a single convection-radiation coefficient [11]. The convective heat transfer at concrete surface can be expressed as

$$q = h(T_s - T_a) \tag{2}$$

Where: q is the convective heat flux per unit area, h is the combined convection-radiation heat transfer coefficient (kcal/m² hr °C), T_s and T_a are the surface and air temperature.

In a real mass concrete footing, heat loss to surrounding air is processed by convection. Normally, the side and bottom faces of the footing are covered by subsoil and heat dissipates from concrete to the surrounding soil by conduction. However, the problem can be simplified by assuming that the amount of heat loss to the surrounding subsoil is assumed to be done by the convection process. This kind of assumption and boundary condition was used in a previous study of other researchers [11]. The model was verified with the test results conducted in the lab and the measured results of many real footings. The verifications were shown in the previous studies of the authors [4]. The verifications show that the model is satisfactory for predicting temperature of the measured footings.

2.1.2 Restrained Strain Analysis

At each time step, the temperature at each position in the mass concrete, obtained from heat transfer analysis, is used as the input for the restrained strain analysis. The internal deformation and stress in each element are related by Hooke's law as shown in Eq. (3).

$$\{\Delta\sigma(t)\} = E(t)[\bar{D}]\{\Delta\varepsilon_{res}(t)\} \tag{3}$$

Where: $\Delta\sigma(t)$ is the change of stress at the considered age (MPa), $\Delta\varepsilon_{res}(t)$ is the restrained strain at the considered age (micron). $E(t)$ is the modulus of elasticity at the considered age (MPa). $[\bar{D}]$ is the material properties matrix and t is the considered age.

In case of the absence of external loading, the stresses that cause cracking of early age concrete are induced by restraint of deformations. In the existing model, the restrained strain in mass concrete is caused mainly from the thermal strain due to the temperature change of concrete. The free thermal strain of concrete element subjected to thermal expansion can be calculated from Eq. (4).

$$\Delta \varepsilon_{th}(t) = CTE(t) \Delta T(t) \quad (4)$$

Where: $\Delta \varepsilon_{th}(t)$ is the free thermal expansion strain. $CTE(t)$ is the coefficient of thermal expansion coefficient (micron/ °C) and $\Delta T(t)$ is the temperature change at the considered age (°C).

2.1.3 Verification of the Model to Predict Thermal Cracking of Mass Concrete

The model was verified with a real concrete footing. Fig.2 shows a thermal crack on one side of the footing. The size of the footing was 14 x 63 x 1.4 m. The footing was cured by insulation curing for 4.6 days. Cracks were found right after the removal of the insulation materials. This means that cracks might have occurred at early age before the removal of the insulation material.

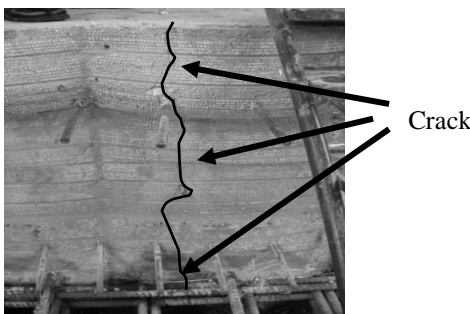


Fig.2. Crack on side surface.

The analytical results of temperature and restrained strain at the core zone at top surface, mid-depth and bottom surface of the

footing are shown in Fig.3 and Fig.4. The rapid change of temperature and restrained strain after 4.6 days occurs due to the removal of insulation material. In terms of temperature, the top surface shows the lowest but mid-depth shows the highest temperature.

The different expansion between mid-depth and surface causes internal restraint between mid-depth and surface of the structure. The surface is restrained in tension and mid-depth part is restrained in compression. The analytical results show the same tendency as that occurs in mass concrete as shown in Fig.4. The restrained strain in tension ($\varepsilon_{res, ten}$) at top surface is the highest. The $\varepsilon_{res, ten}$ at top surface obtained from the analysis is compared with the authors' tested tensile strain capacity of concrete (TSC) and if the $\varepsilon_{res, ten}$ is higher than tensile strain capacity then the mass concrete structure is predicted to crack.

Fig.4 shows the comparison between the predicted $\varepsilon_{res, ten}$ on the top surface and TSC of the concrete. By comparing the analyzed restrained strain with the authors' test results of TSC [5], the footing was predicted to crack at early age before the removal of the insulation material. From the comparison using the authors' proposed model and tested TSC, it can be concluded that the model was satisfactory to predict thermal cracking of the footing.

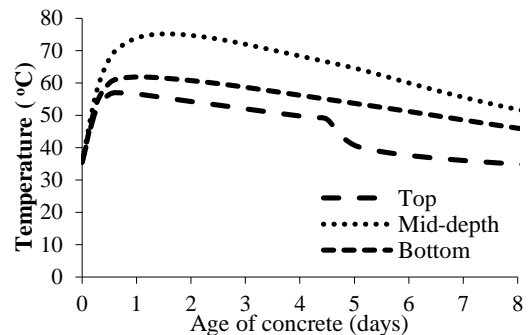


Fig.3. Predicted temperatures at top, center and bottom parts.

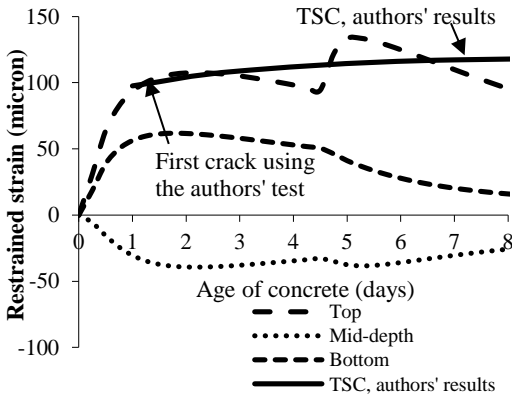


Fig.4. Comparison between tensile strain capacity and predicted restrained strain in lateral direction.

2.2 Shrinkage Model

In this study, the authors' previously proposed models for predicting free shrinkage of concrete is used in the analysis. Details of the models are given in [5]. Total shrinkage of concrete is the summation of autogenous shrinkage and drying shrinkage which can be calculated by using Eq. (5). When calculating the total shrinkage, curing period (t_0) and type of curing must be considered because they affect values of autogenous shrinkage and drying shrinkage. In the case of water-cured concrete, water can penetrate continuously resulting in insignificant autogenous shrinkage and drying shrinkage during the water curing period especially for thin concrete members. In the case of seal-cured or moist-cured (wet burlap) concrete, there is no water or insufficient water, respectively, supplied into the concrete. Therefore, autogenous shrinkage can occur during the seal curing or moist curing period while there is no drying shrinkage because of no drying on concrete surface. In this condition, the total shrinkage includes the autogenous shrinkage from the time of final setting to the time considered. More details of the autogenous shrinkage model and drying shrinkage model are mentioned in sections 2.2.1 and 2.2.2, respectively.

$$\varepsilon_{TS}(t, t_0) = \varepsilon_{as}(t, t_0) + \varepsilon_{ds}(t, t_0) \quad (5)$$

Where:

$\varepsilon_{TS}(t, t_0)$ = total shrinkage strain from age of t_0 to t (micron)

$\varepsilon_{as}(t, t_0)$ = autogenous shrinkage strain from age of t_0 to t (micron)

$\varepsilon_{ds}(t, t_0)$ = drying shrinkage strain from age of t_0 to t (micron)

T = time considered (days)

t_0 = age at start of drying of concrete (days)

2.2.1 Autogenous Shrinkage Model

Unrestrained autogenous shrinkage was calculated by using a two-phase model concept shown in Eq. (6) for computing concrete autogenous shrinkage strain. Shrinkage occurs only in the paste phase whereas the aggregate phase is considered to restrain the paste shrinkage because of particle interaction. A two-phase material model shown in Eq. (7), taking into account the restrained shrinkage due to aggregate particle interaction proposed by Tatong, 2001 [14], was adopted in this analysis. This model involved the stiffness, equilibrium condition and strain compatibility of paste phase and aggregate phase.

$$\varepsilon_{as}(t, t_0) = \varepsilon_{as}(t) - \varepsilon_{as}(t_0) \quad (6)$$

$$\varepsilon_{as}(t) = \frac{\varepsilon_{po}(t) \cdot E_p(t) \cdot (1 - n_a)}{E_p(t) + E_a} \quad (7)$$

Where: $\varepsilon_{as}(t, t_0)$ is the autogenous shrinkage strain from age t_0 to t (micron), $\varepsilon_{po}(t)$ is the free shrinkage of paste in concrete at the considered age (micron). n_a is the volume concentration of aggregate. $E_p(t)$ is stiffness of paste phase at considered age (kg/cm^2). E_a is stiffness of aggregate phase (kg/cm^2). t_0 is the age at start of drying of concrete (days) and t is the considered age (days).

2.2.2 Drying Shrinkage Model

Unrestrained drying shrinkage was calculated by using Eqs. (8) to (11). The drying shrinkage model takes into account the effect of cement type, fly ash, water to binder ratio, paste content, curing condition, ambient relative humidity and volume to surface area ratio[13]. All of these parameters significantly affect the drying shrinkage of concrete.

$$\varepsilon_{ds}(t, t_0) = \varepsilon_{dsm} \cdot \beta(t, t_0) \cdot \beta(h) \quad (8)$$

$$\varepsilon_{dsm} = \left(663 - 291 \exp\left(-7.26 \left(\frac{w}{b}\right)^{5.26}\right) \right) \cdot K_1 \cdot K_2 \cdot K_3 \cdot K_4 \quad (9)$$

$$\beta(h) = 1.73 \left(1 - \left(\frac{RH}{100} \right)^3 \right) \quad (10)$$

$$\beta(t, t_0) = \left[\frac{(t - t_0) \cdot B \cdot P}{(t - t_0) + A \cdot G \cdot N \cdot F} \right] \quad (11)$$

Where: $\varepsilon_{ds}(t, t_0)$ is the drying shrinkage strain of concrete from age t_0 to t (micron). ε_{dsm} is drying shrinkage strain of concrete at 150 days of age (micron). $\beta(h)$ is a factor for considering the effect of relative humidity. $\beta(t, t_0)$ is the time-dependent function component. K_1 , K_3 and K_4 are factors considering the effect of the volume concentration of aggregate, fly ash content, and curing condition (curing type and curing period), respectively. K_2 and P are coefficients for cement type. A and B are factors considering the effect of strength of concrete. G is a factor considering the effect of volume to surface ratio. N and F are factors considering the effect of aggregate content and fly ash content. RH is relative humidity (%). t_0 is the age at start of drying of concrete (days) and t is the considered age (days).

Verification of the total shrinkage model was performed on concrete specimens exposed to drying condition. Experiments were conducted on concrete with different water to binder ratios, fly ash content, paste content, curing period and curing type. The results obtained from total shrinkage tests by

the authors' research group and data obtained from various researchers were compared with the model of total shrinkage of concrete. An example of verification is shown in Fig.5. It was found that the results obtained from the model were in good agreement with the experimental results [5].

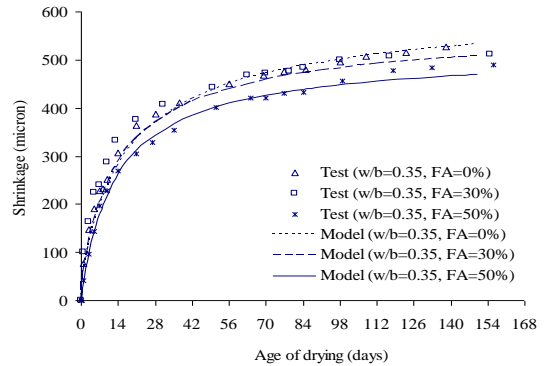


Fig.5. Comparisons between test results of total shrinkage of concrete and the computed results from the model of concrete with various replacement percentages of fly ash with w/b of 0.35, $n_a=0.676$, temperature=28°C, RH=75% (water curing=7 days)[5].

3. Modification of Existing Models

3.1 Mechanisms of Cracking due to Heat of Hydration and Shrinkage in Mass Concrete

As shown in Figs.6 and 7, for internal restraint the restrained strain of mass concrete is contributed from the thermal strain and shrinkage strain. The restrained strain caused by thermal strain in mass concrete is in compression at the inner core and in tension at the surface, leading to the risk of thermal cracking. The restrained strain caused by shrinkage strain was separated into two parts. In the first part, autogenous shrinkage strain is the strain that occurs in the whole body of the mass concrete. Based on degree of hydration, the highest autogenous shrinkage strain occurs in the center part which has the highest degree of hydration reaction. The second part is the drying shrinkage strain that takes place on the exposed surfaces of the mass concrete. The effect of drying shrinkage exists up to a

depth that has no moisture loss. The resulting restrained strain in mass concrete is derived by superimposing the thermal and shrinkage strains as shown in Eqs. (12) and (13).

$$\varepsilon_{res}(t) = \varepsilon_{res,sh}(t) + \varepsilon_{res,th}(t) \tag{12}$$

$$\varepsilon_{res,sh}(t) = \varepsilon_{res,as}(t) + \varepsilon_{res,ds}(t) \tag{13}$$

Where: $\varepsilon_{res}(t)$ is the restrained strain resulting from thermal and shrinkage effects, while $\varepsilon_{res,th}(t)$, $\varepsilon_{res,sh}(t)$, $\varepsilon_{res,as}(t)$ and $\varepsilon_{res,ds}(t)$ are the restrained strains of concrete by thermal effect, by total shrinkage, by autogenous shrinkage and by drying shrinkage at the considered age, respectively, (micron) and t is the considered age (days).

In general, at early age, insulation curing is recommended to be used for mass concrete for the benefit of temperature control. During this stage there is no loss of water to the surrounding environment; in other words, drying shrinkage is insignificant during this stage and it is neglected during the insulation curing period. After the removal of insulation materials, there is loss of water at the concrete surface due to evaporation; as a result both autogenous shrinkage and drying shrinkage are considered.

However, in this study, the analysis mainly focuses on the strain that occurs during the first 7 days when the mass concrete is cured by using the insulation curing method. The stage after curing is not included in this paper and it will be described in the future study.

An existing model to predict semi-adiabatic temperature and thermal cracking in mass concrete proposed by Choktaweekarn [4] was used in this study. It was modified to take into account the effect of shrinkage in mass concrete. The free shrinkage strain used in the analysis is calculated by using the model proposed by Tongaroonsri [5], as shown in Eqs. (12) to (13). The calculated temperature of concrete at each position is

used as the input in the shrinkage model to calculate the autogenous shrinkage at each position. As shown in Fig. 6, the autogenous shrinkage at the mid-depth of mass concrete is higher than at the top surface. This is because when the temperature at the mid-depth of mass concrete is higher than the surface, the degree of hydration at mid-depth is higher. For this reason, based on degree of hydration, autogenous shrinkage strain at the mid-depth is higher than that at the concrete surface. The free shrinkage strain at each position was input into the FEM program in the form of temperature change as shown in Eq. (14).

$$\Delta T_{sh}(t) = \varepsilon_{sh}(t) / CTE(t) \tag{14}$$

Where: $\varepsilon_{sh}(t)$ is the input free shrinkage strain at the considered age (micron). CTE(t) is the coefficient of thermal expansion coefficient (micron/°C) and $\Delta T_{sh}(t)$ is the shrinkage equivalent temperature change at the considered age (°C) and t is the considered age (days).

In the restrained strain analysis, the restrained strains from thermal and shrinkage effects are analyzed separately. At the end of the analysis, both restrained strains are superimposed as illustrated in Fig.6 and Fig.7.

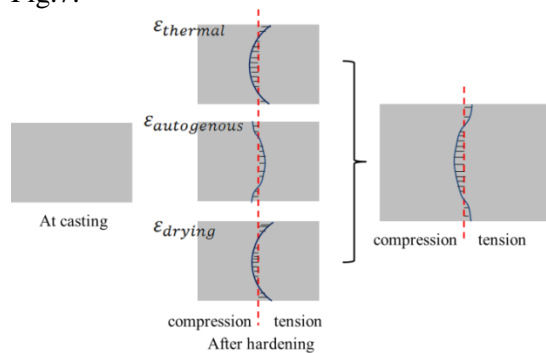


Fig.6. Strain distributions of mass concrete.

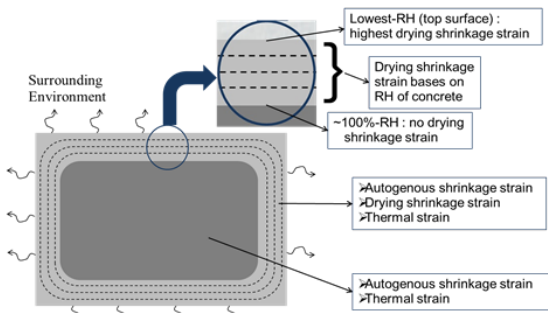


Fig.7. Type of restrained strain in different parts of the mass concrete.

4. Analytical Results

A concrete block with a size of 5.5 x 11 x 2.5 m was used as an example to simulate the effect of shrinkage on mass concrete (Fig.8). This concrete block was assumed to be cured by insulation curing for 7 days. Mix proportion and 28-day compressive strength of concrete used in the analysis are shown in Table1.

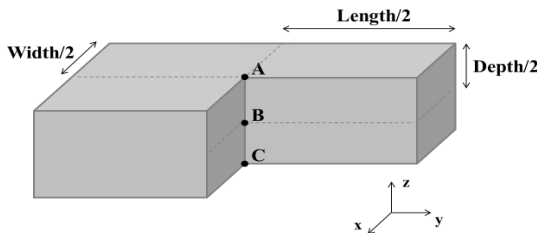


Fig.8. An example concrete block.

Table1. Mix proportion of concrete (in kg/m³).

Cement	Water	Sand	Gravel	28-day Compressive Strength (MPa)
294	150	860	1123	25.8

A flow chart of the analytical process for simulating cracking of mass concrete is shown in Fig.9. The adiabatic temperature was obtained when knowing mix proportion. Concrete mix proportion and properties of cementitious materials were used for calculating adiabatic temperature. Predicted adiabatic temperature is shown in Fig.10.

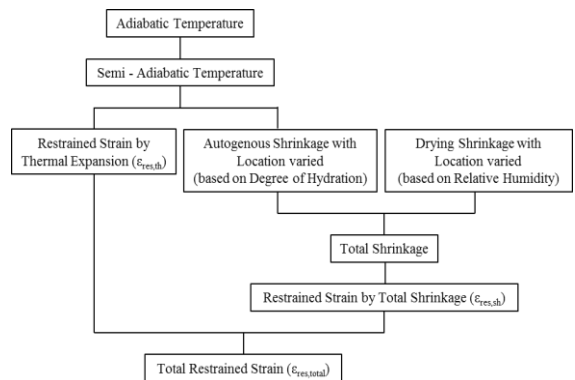


Fig.9. A flow chart of the analysis for simulating cracking of mass concrete.

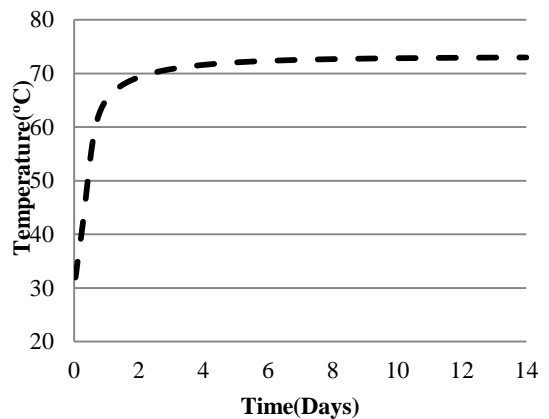


Fig.10. Predicted adiabatic temperature.

Thermal properties such as specific heat, thermal conductivity and cumulative heat generation, dimension of structure, ambient temperature, boundary conditions and convection heat transfer coefficient were used as the inputs to analyze the semi-adiabatic temperature rise of concrete. Predicted semi-adiabatic temperatures are shown in Fig.11. The results in Fig.11 show that the temperature at location B (mid-depth) is higher than that at location A and C (the top and the bottom surfaces, respectively).

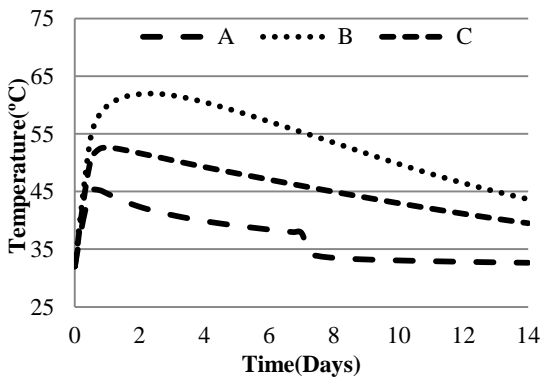


Fig.11. Predicted semi-adiabatic temperatures at location A, B and C (top, mid-depth and bottom surfaces, respectively).

From Fig.11, the temperature gradients between center and surface of concrete were used to analyze the restrained strain due to differential thermal deformation where modulus of elasticity, Poisson’s ratio and coefficient of thermal expansion were used as the input of the computation. Restrained thermal strains at locations A, B and C in Fig.8 of concrete are shown in Fig.12.

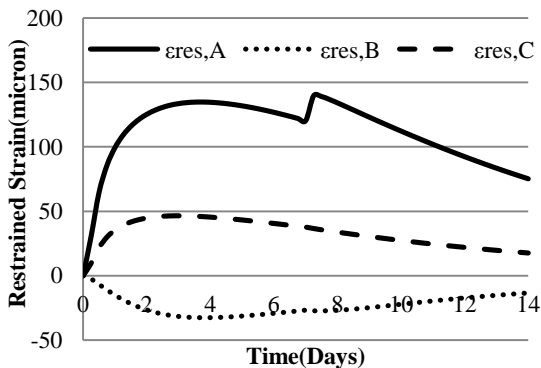


Fig.12. Restrained thermal strain at surface of concrete.

Fig.12 shows the restrained strain without effect of shrinkage consideration. $\epsilon_{res,A}$, $\epsilon_{res,B}$ and $\epsilon_{res,C}$ are restrained thermal strains at locations A, B and C, respectively. The restrained strain by thermal expansion at the surface of concrete shows two peak values, one at early age and another at the day the insulation curing material is removed (7 days), and after that the value decreases

continuously. It should be noted that the effect of shrinkages in the 2nd peak (at the time of insulation material removal is not discussed. The target is to demonstrate the effect of autogenous shrinkage at the early age (before insulation material removal) and drying shrinkage after drying exposure (after removing the insulation material). At the point of insulation material removal, the effect of autogenous shrinkage is smaller than that at the earlier age. Also, the effect of drying shrinkage is still not seen at that time since the concrete surface has just been exposed to drying.

To consider the effect of restrained strain by shrinkage, free shrinkage strains were used as input at each location. Firstly, the differential autogenous shrinkage came from the effect of temperature gradient in Fig.11. These temperatures were used to compute the degree of hydration, which affects autogenous shrinkage as shown in Fig.13. It can be seen that the inner portion (B) is in tension while the near surface portions (A and C) are in compression because the inner portion with higher temperature has higher autogenous shrinkage. The inner portion is in self-equilibrium with the lower autogenous shrinkage portion near the surface.

The analytical results of restrained strain at mid-depth (B) and surface (A) are shown in Fig.14. Fig.14 shows that autogenous shrinkage strain at the mid-depth is higher than that near the top surface due to higher temperature and degree of hydration, while the lowest autogenous shrinkage at the top surface is due to lower temperature and moisture content (due to drying near the exposed surface), leading to lower degree of hydration reaction, especially at the early age.

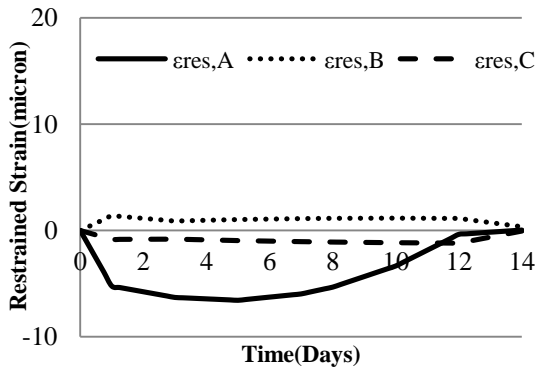


Fig.13. Restrained autogenous shrinkage strains.

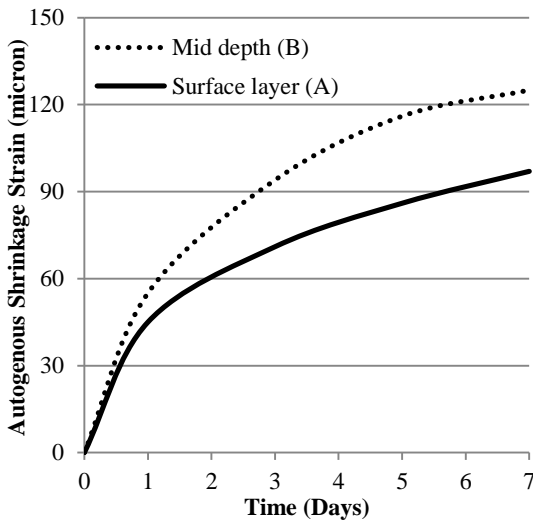


Fig.14. Different autogenous shrinkage at mid-depth (location B) and surface layer (location A) due to different degree of hydration.

The analytical results at mid-depth and top surface at the section center were used in the discussions. The free shrinkage strain at each position was input into the FEM program in the form of temperature change as shown in Eq. (14). The restrained autogenous shrinkage strain was computed separately as shown in Fig.13 and the summation of the restrained strains by thermal and autogenous shrinkage effects are shown in Fig.15.

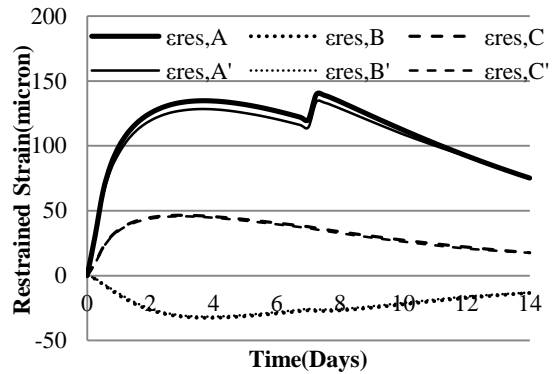


Fig.15. Combined restrained thermal and autogenous strains.

$\epsilon_{res,A'}$, $\epsilon_{res,B'}$ and $\epsilon_{res,C'}$ are the combined restrained thermal-autogenous shrinkage strain at locations A, B and C, respectively. It can be seen from Fig.15 that the combination of the autogenous shrinkage strain with thermal strain results in reduction of restrained strain near the top surface of the concrete (comparing $\epsilon_{res,A}$ with $\epsilon_{res,A'}$). The restrained strain by only thermal strain ($\epsilon_{res,A}$) is reduced by about 10 micron by the restrained autogenous shrinkage strain. The restrained total shrinkage strain was also computed separately as shown in Fig.16. Free total shrinkage strain in Fig.17 was used as input at each location.

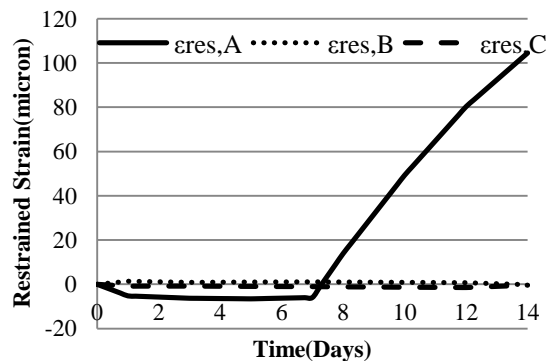


Fig.16. Restrained total shrinkage strains.

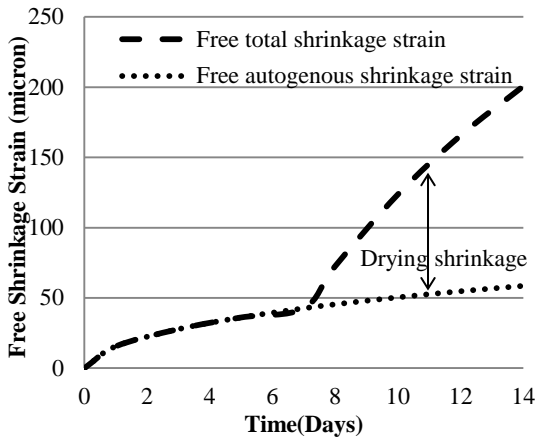


Fig.17. Free total shrinkage strains at the top surface of concrete.

Fig. 17 shows the restrained strain caused by total shrinkage (summation of autogenous and drying shrinkages). Autogenous shrinkage reduces restrained strain during the insulation curing period but drying shrinkage increases restrained strain of the mass concrete after the insulation curing period. It was assumed that there was no drying shrinkage during the insulation curing period.

After combining restrained strain due to total shrinkage with thermal restrained strain, the net restrained strains in Fig.18 decrease at early age because of autogenous shrinkage. After insulation curing material is removed (7 days), restrained drying shrinkage strain shows great effect on the tension zone and leads to cracking at the mass concrete surface when the net restrained strain is greater than tensile strain capacity (TSC in Fig.18). It is therefore recommended not to let the exposed surface of concrete dry immediately after the removal of insulation.

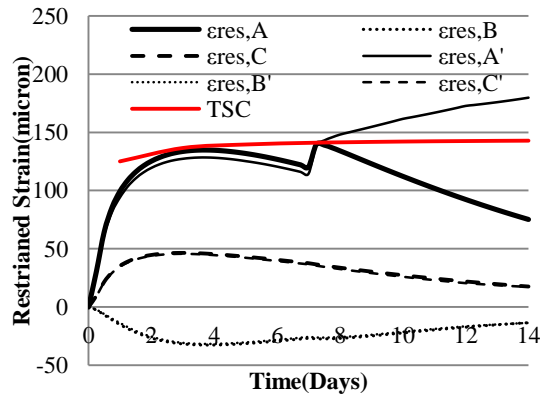


Fig.18. The net restrained strains.

The consideration of autogenous and drying shrinkages will result in a more realistic prediction of cracking in mass concrete footings. It was found that the effect of drying shrinkage is more significant than the effect of autogenous shrinkage for the internally restrained thermal stress. It's noted that creep and relaxation are not included in this study. For future study, the effect of creep and relaxation of concrete might be included to the computation for more precise prediction.

5. Conclusion

From the analytical results, it was found that autogenous shrinkage reduces the risk of cracking especially at the early age before the removal of insulation curing material. However mass concrete can be at risk by the effect of drying shrinkage after the removal of the insulation curing material. Care must be taken to prevent excessive loss of moisture.

6. Acknowledgement

The authors would like to acknowledge the Center of Excellence in Material Science, Construction and Maintenance Technology Project, and the National Research University Project, Office of the Higher Education Commission.

7. References

- [1] Schutter, G.D., Finite Element Simulation of Thermal Cracking in Massive Hardening Concrete Elements Using Degree of Hydration Based Material Laws, Computers and Structures, Vol. 80, pp.2035-2042, 2002.
- [2] Kim J.K., Kim K.H. and Yang J.K., Thermal Analysis of Hydration Heat in Concrete Structures with Pipe-cooling System, Computers and Structures, Vol. 79, pp.163-171, 2002.
- [3] Noorzaei J., Bayagoob K.H., Thanoon W.A. and Jaafar M.S., Thermal and Stress analysis of Kinta RCC Dam, Engineering Structures, Vol. 28, pp. 1795–1802, 2006.
- [4] Choktaweekarn P., Thermal Properties and Model for Predicting Temperature and Thermal Cracking in Mass Concrete, Doctoral Thesis, Sirindhorn International Institute of Technology, Thammasat University, Thailand, 2008.
- [5] Tongaroonsri S., Prediction of Autogenous Shrinkage, Drying Shrinkage and Shrinkage Cracking in Concrete, Doctoral Thesis, Sirindhorn International Institute of Technology, Thammasat University, Thailand, 2009.
- [6] Saengsoy W. and Tangtermsirikul S., Model for Predicting Temperature of Mass Concrete, Proceedings of The 1st National Concrete Conference, Engineering Institute of Thailand, Kanchanaburi, May 2003, pp.211-218.
- [7] Kwak, H.G., Ha S.J. and Kim J.K., Non-structural Cracking in RC Walls: Part I. Finite Element Formulation, Cement and Concrete Research, Vol. 36 No.4, pp.749-760, 2006.
- [8] Sarker P.K., Jitvutikrai P., Tangtermsirikul S. and Kishi T., Modeling of Temperature Rise in Concrete Using Fly Ash, Concrete Model Code for Asia IABSE Colloquium, Phuket, Thailand, pp. 126-132, 1999.
- [9] Maekawa K., Chaube R. and Kishi T. Modelling of Concrete Performance, E & FN Spon, London, 1999.
- [10] Wang C. and Dilger W.H., Prediction of Temperature Distribution in Hardening Concrete, in: Springenschmid R. (Ed.), Thermal Cracking in Concrete at Early Ages, E & FN Spon, London, UK, pp 21-28, 1994.
- [11] Faria R., Azenha M. and Figueiras J.A., Modelling of Concrete at Early Ages: Application to an Externally Restrained Slab, Cement and Concrete Composites, Vol. 28, No. 6, pp.572-585, 2006.
- [12] Sicat E., Gong F., Zhang D., and Ueda T., Change of the Coefficient of Thermal Expansion of Mortar Due to Damage by Freeze Thaw Cycles, Journal of Advanced Concrete Technology Vol.11, pp.333-346, 2013.
- [13] Maruyama I., and Igarashi G., Cement Reaction and Resultant Physical Properties of Cement Paste, Journal of Advanced Concrete Technology, Vol.12, pp. 200-213, 2014.
- [14] Tatong S., and Tangtermsirikul S., Modeling of Aggregate Stiffness and Its Effect on Shrinkage of Concrete, Science Asia, Vol.27, No. 3, pp.185-192, 2001.